Food Chemistry 277 (2019) 273–278

Contents lists available at ScienceDirect

Food Chemistry

journal homepage: www.elsevier.com/locate/foodchem

Sensitive aptamer-based fluorescene assay for ochratoxin A based on RNase H signal amplification

Kefeng Wu, Changbei Ma*, Han Zhao, Mingjian Chen, Zhiyi Deng

School of Life Sciences, Central South University, Changsha 410013, China

ARTICLE INFO

Keywords:
Fluorescence
Ochratoxin A
RNase H
Signal amplification

ABSTRACT

A new assay for the selective and sensitive aptamer-based fluorescent biosensor for ochratoxin A (OTA) detection is proposed. It consists of a ribonuclease H (RNase H)-assisted cycle response that leads to a significant amplification of the signal, which allow for a low limit of detection (LOD) of 0.08 ng/mL. By using this technique, a high selectivity for OTA against ochratoxin B and aflatoxin B_1 (AFB_1) was noticed. The quantitative determination in real samples has been verified using red wine samples spiked with a series of OTA concentrations (0.4, 4, and 12 ng/mL), and the recoveries ranged from 96.1 to 107.5%. This aptasensor has great practical applications in food industry and moreover, can be extended for the detection of other toxins by replacing the sequence of the recognition aptamer.

1. Introduction

Ochratoxin A (OTA), a major food-contaminating mycotoxin, is found in various kinds of agricultural products, such as cereals, coffee, cocoa, dried fruits, wine, grape juice, beer, spices, meat, and meat products (Ahmed, Farag, Soliman, Abdel-Samed, & Naguib, 2007; Alonso-Lomillo, Domínguez-Renedo, Román, & Arcos-Martínez, 2011; Assaf, Azouri, & Pallardy, 2004; Bennett & Klich, 2003). OTA, which is commonly detected in microorganisms is a fungal secondary metabolite of high toxicity (Ghali, Hmaissia-Khlifa, Ghorbel, Maaroufi, & Hedili, 2008, 2009; Imperato, Campone, Piccinelli, Veneziano, & Rastrelli, 2011; Van, Steyn, Fourie, Scott, & Theron, 1965). In humans or animals, excessive OTA can negatively influence the protein synthesis, enhance the lipid peroxidation, harm the saccharide and calcium metabolisms, and paralyse the mitochondrial functions (Costa et al., 2016; Zhang et al., 2016).

The potential human health risks of OTA exposure are related to a variety of toxic effects, such as nephrotoxic, hepatotoxic, immunotoxic, teratogenic, and carcinogenic effects (Khoury & Atoui, 2010). Furthermore, OTA potentially suppresses the immune system as a result of the atrophy of the immune organs (Boorman et al., 1984), slowing down the reaction of antibody, disturbing the modification in immune cell activities (Muller, Burkert, & Rosner, 2003), and adjusting the cytokine production (Lea, Steien, & Størmer, 1989). More importantly, OTA is very stable and it has a long half-life of 35.5 days, which result in an accumulation of the toxin into the body (Studerrohr, Schlatter, & Dietrich, 2000). Besides, it can be quickly absorbed, but hard to degrade. Due to its so harmful effects, OTA is listed as potentially carcinogenic compound by the International Agency for Research on Cancer (IARC) (International Agency on Research on Cancer, 1993). So far, systematic regulations on the management of OTA were globally accepted and great efforts have been made to develop simple but efficient methods to detect it. Song et al. reported a label-free and sensitive detection of Ochratoxin A based on dsDNA-templated copper nanoparticles and exonuclease-catalyzed target recycling amplification (Song, Hong, Zhang, & Lu, 2018). Liu et al. developed a fluorometric aptamer based assay for ochratoxin A based on the use of exonuclease III (Liu et al., 2018). Zejli et al. proposed a label free aptasensor for ochratoxin A detection using polythiophene-3-carboxylic acid (Zejli, Yugender Goud, & Marty, 2018). Although these methods could detect OTA, the LOD are poor and linear ranges are relatively narrow. Therefore, it is still necessary to develop efficient and sensitive methods for OTA monitorization while keeping in mind the guarantee of food safety by eliminating the potential risk caused by OTA consumption.

Traditional methods of OTA analysis include thin-layer chromatography (TLC), high-performance liquid chromatography (HPLC), gas chromatography (GC), and mass spectrometry (MS) (Songsermsakul & Razzazi-Fazelib, 2008; Turner, Subrahmanyam, & Piletsky, 2009). However, shortcomings like time-consuming, expensiveness and inaccuracy are related to these methods. Besides, immunological methods, especially enzyme-linked immunosorbent assay (ELISA) (Liu, Tsao, Wang, & Yu, 2008), have been employed in OTA assay. However,

* Corresponding author.
E-mail addresses: kefeng@csu.edu.cn (K. Wu), macb2012@csu.edu.cn (C. Ma), 172511001@csu.edu.cn (H. Zhao), chenmingjian@csu.edu.cn (M. Chen).

https://doi.org/10.1016/j.foodchem.2018.10.130
Received 26 May 2018; Received in revised form 6 October 2018; Accepted 28 October 2018
Available online 29 October 2018

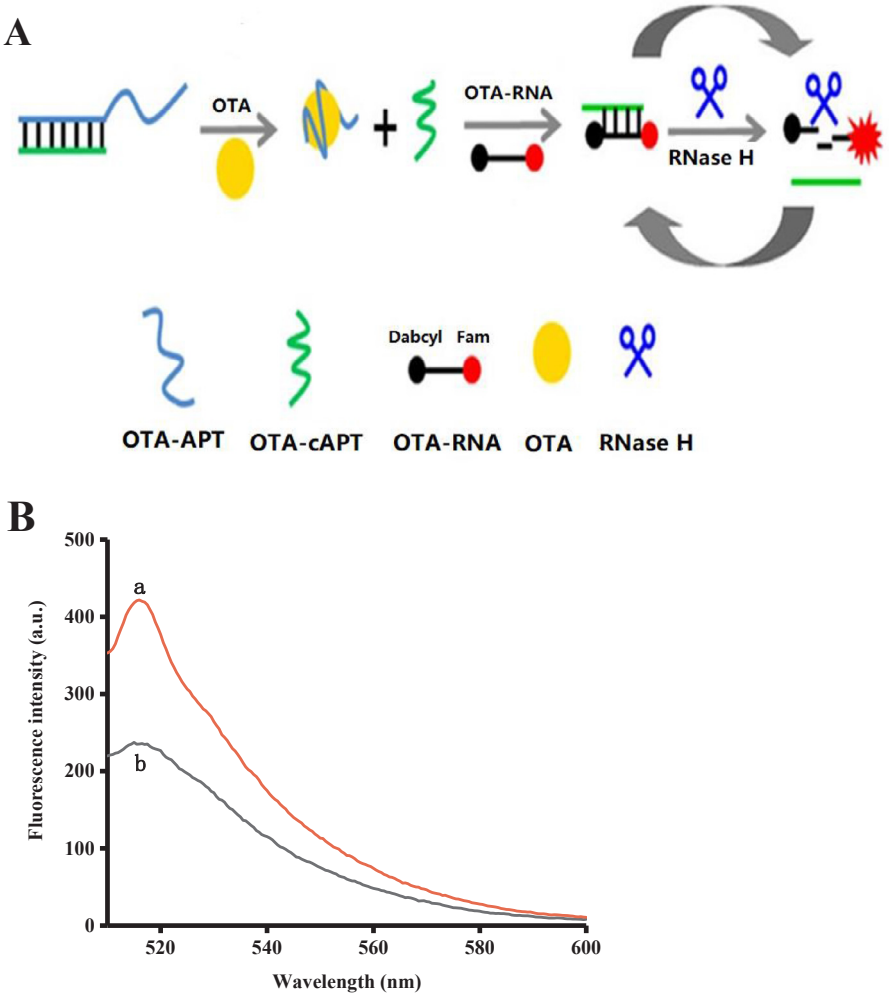

Fig. 1. (A) Schematic illustration of the fluorescent aptamer sensor for OTA; (B) fluorescence spectra of aptameric assay system in the absence (b) and presence (a) of OTA.

ELISA requires the use of antibodies which were greatly affect by environmental temperature and pH, the pretreatment process of ELISA is costly and complicated.

Aptamers are single-stranded nucleic acids or peptide molecules exhibiting unique secondary structures that can bind specifically to their targets (Guo & Zhao, 2016; Tong, Zhao, Zhang, Xu, & Chen, 2012). Due to their ability to bind to a larger number of targets such as small molecules, proteins, nucleic acids, cells, tissues, and organisms, an aptamer can be easily utilized (Cho, Lee, & Ellington, 2009; Li, Zhao, Chen, Mu, & Guo, 2011; Yang, Lates, Prieto-Simón, Marty, & Yang, 2012). To date, a series of aptamer-based methods for OTA detection have been reported, among them a fluorescence assay (Chen, Fang, Liu, & Zeng, 2012; Lv, Li, Cui, Zhao, & Guo, 2017; Mckeague et al., 2014; Wang et al., 2016), an electrochemical assay (Mayorga-Martinez, Quesada-González, Zamora-Gálvez, de la Escosura-Muñiz, & Merkoçi, 2015; Mishra, Hayat, Catanante, Istamboulie, & Marty, 2016), a colorimetric assay (Lee, Jeon, Ahn, & Ha, 2014; Luan et al., 2015; Yin et al., 2017), and a photoelectrochemical immunosensor based assay (Feng et al., 2018). These assays, involving a binding ratio between aptamers and targeted molecules of 1:1, usually fail in amplifying the signal, and thus, a low sensitivity in the OTA detection is reported. Hence, a strategy that involves an OTA-specific aptamer is required to improve the detection limit and selectivity for OTA. Here, the use of RNase H was explored due to its ability to specifically cleave the RNA strand of DNA/RNA hybrid. To the best of our knowledge, this RNA based aptasensor is used for the first time to detect OTA. Moreover, we demonstrated that the RNase H platform can be successfully used for highly selective and sensitive fluorescence detection of OTA.

2. Experimental

2.1. Materials and methods

Ochratoxin A (OTA) and ochratoxin B (OTB) were purchased from Pribolab Co., Ltd (QingDao China). Aflatoxin B_1 (AFB_1) was purchased from Yuanye Co., Ltd (ShangHai China). Ribonuclease H (RNase H) and labeled RNA probe (OTA-RNA: 5′-FAM-GAUCGGGUGUGG-Dabcyl-3′) were obtained from Takara Biotechnology Co., Ltd (DaLian, China). DNA probes (OTA-APT: 5′-GATCGGGTGTGGGTGG CGTAAAGGGAGC ATCGGACA-3′, and OTA-cAPT: 5′-CGCCACCCACACCC GATC-3′) were purchased from Sangon Biotechnology Co., Ltd (Shanghai, China). All experiments were repeated three times, and error bars were calculated by Origin software.

2.2. Optimization of the experimental conditions

All experimental conditions were optimized, including the ratio of OTA-APT:OTA-cAPT, the concentrations of OTA-cAPT and OTA-RNA probes. The experiments were performed for a ratio range of OTA-APT:OTA-cAPT from 5 to 1. The OTA-cAPT probe concentrations were 10, 30, 50, 70, and 100 nM. The concentrations of OTA-RNA probe were 100, 200, 300, 400, and 500 nM.

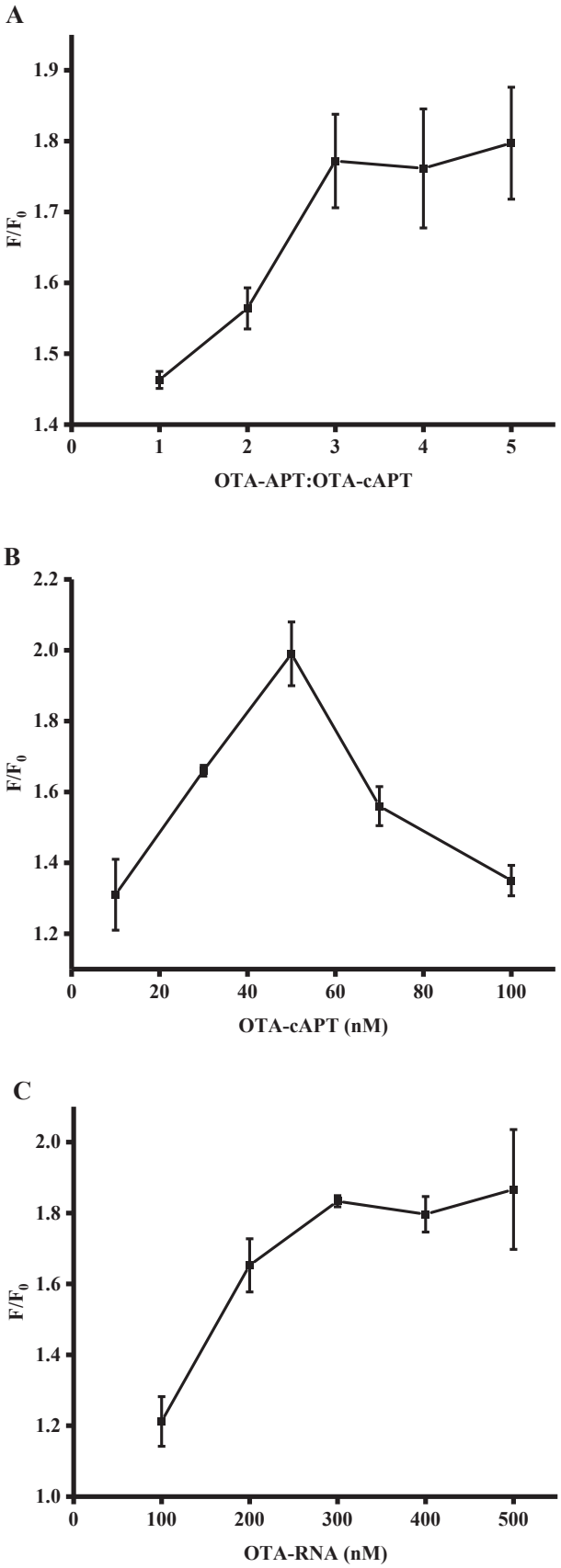

Fig. 2. Optimization experimental conditions of OTA detection: (A) ratio of OTA-APT/OTA-cAPT; (B) concentration of OTA-APT probe; (C) concentration of OTA-RNA probe. F_0 and F represent the fluorescence intensities in the absence and presence of OTA. Error bars were estimated from three replicate measurements.

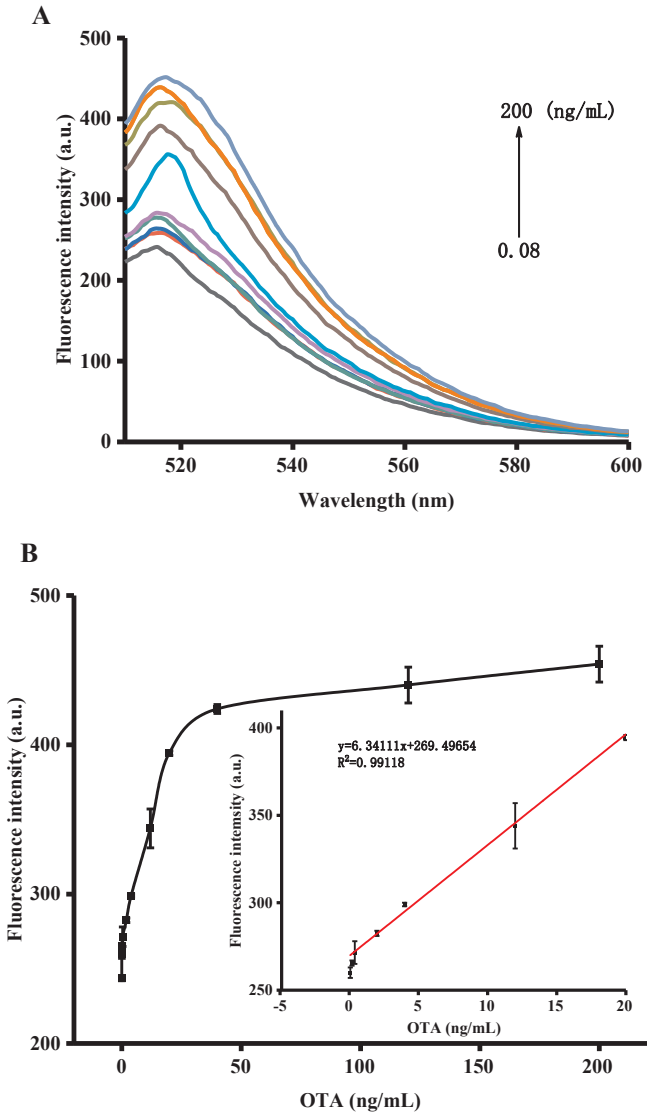

Fig. 3. (A) Fluorescent signal response with different concentrations of OTA. OTA concentration increased from bottom to top: 0.08, 0.2, 0.4, 2, 4, 12, 20, 40, 120 and 200 ng/mL; (B) calibration curve with the linear portion inserted. OTA-cAPT = 50 nM, OTA-APT = 150 nM, OTA-RNA = 300 nM, RNase H = 12 U, Temperature = 25 °C. Error bars were estimated from three replicate measurements.

Table 1
Comparison with the currently reported methods for OTA determination.

Method	Detection limit (ng/mL)	Linear range (ng/mL)	Reference
Colorimetric	8	8–250	Yin et al. (2017)
Colorimetric	0.4	–	Lee et al. (2014)
Electrochemical	0.07	0.15–5	Mishra et al. (2016)
Chemiluminescence	0.22	0.1–100	Jo, Mun, Kim, Shim, and Kim (2016)
UV–vis	0.22	0.5–20	Xu, Xu, and Ying (2016)
Fluorescence	0.8	1–100	Chen et al. (2012)
Fluorescence	4	4–80	Lv et al. (2017)
Fluorescence	0.08	0.4–20	This work

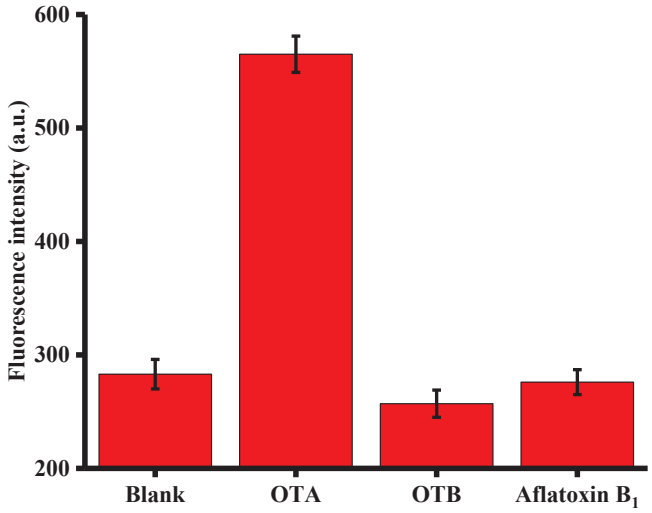

Fig. 4. Selectivity of the sensor toward OTA against OTB and Aflatoxin B_1. OTA-cAPT = 50 nM, OTA-APT = 150 nM, OTA-RNA = 300 nM, RNase H = 12 U, Temperature = 25 °C, OTA = OTB = AFB_1 = 200 ng/mL. Error bars were estimated from three replicate measurements.

Table 2
Application of aptasensor for OTA determination in red wine.

Sample	Added (ng/mL)	Found (ng/mL)	Recovery (%)
Sample 1	0.4	0.41 ± 0.16	103
Sample 2	4	4.30 ± 0.26	107.5
Sample 3	12	11.54 ± 0.50	96.1

2.3. Aptamer biosensor for detecting OTA

For a typical OTA fluorescence experiment, OTA solutions with different concentrations of OTA and buffered at pH = 7.5 (10 mM Tris-HCl, 120 mM NaCl, 20 mM $CaCl_2$, 40 Mm $MgCl_2$), 50 nM OTA-cAPT, and 150 nM OTA-APT were incubated at 25 °C for 30 min. Then, 300 nM OTA-RNA probe and 0.2 μL of RNase H (60 U/μL) were added at 25 °C and allowed to react for 60 min. All experiments were conducted at a final reaction volume of 100 μL. Each experiment was performed three times. Afterwards, the fluorescence was measured as described above. Fluorescence spectra were obtained using a Hitachi F-2700 fluorescence spectrophotometer (Hitachi Ltd, Japan). The samples were placed in quartz cuvettes and excited at 497 nm while the emission spectra were collected at wavelengths ranging from 510 to 600 nm at room temperature.

2.4. Selectivity assay

In order to explore the specificity of the proposed assay, OTB and AFB_1 were used for comparison. First, OTA buffered at pH = 7.5 and 50 nM OTA-cAPT, 150 nM OTA-APT, and 200 ng/mL OTA, OTB and AFB_1 were incubated at 25 °C for 30 min. Then, 300 nM OTA-RNA probe and 0.2 μL of RNase H (60 U/μL) were added at 25 °C and allowed to react for 60 min. Afterwards, the fluorescence was measured as described above.

2.5. Determination of OTA in red wine samples

In order to prove the feasibility of this method in real samples, red wine was used for tests. Before analysis, the red wine samples were filtrated to remove sediments, adjusted to pH = 7.5 and then a 20-fold dilution was applied (Wang, Zhang, Pang, Zhang, & Guo, 2017). Three different concentrations of OTA (0.4, 4, and 12 ng/mL) were spiked into the red wine samples to obtain standard samples. The subsequent manipulation is according to the Section 2.3.

3. Results and discussion

3.1. The operation principle of the developed aptasensor

In this assay, a sensitive and selective RNase H-assisted fluorescence aptamer-based fluorescent biosensor for OTA detection is proposed and the operating principle of this novel sensor is illustrated in Fig. 1A. OTA-APT is the aptamer of OTA and partially complementary with OTA-cAPT. In the presence of OTA, OTA-cAPT is removed from the OTA-APT/OTA-cAPT hybrid duplex and then, combined with OTA-RNA which has a fluorophore on the 3′-end and a quencher at the 5′-end to form DNA/RNA junctions. Since RNase H is an enzyme selective for hydrolysis of RNA in a DNA/RNA hybrid duplex (Wu et al., 2017), the fluorophore and quencher are released from OTA-RNA, showing obvious fluorescence. However, without OTA, the fluorophore and quencher labeled OTA-RNA remains as a single strand. Because the fluorophore and quencher are situated in close proximity, the fluorophore is quenched and emits fluorescence of low intensity. The emitted fluorescence is clear evidence that OTA can be detected by this simple and convenient approach. As shown in Fig. 1B, the sensor produces a significant fluorescence enhancement for the solution containing 200 ng/mL OTA in comparison with a blank.

3.2. Optimization of experimental conditions for the sensing tests

In order to obtain a desirable fluorescence response, the experimental conditions, in particular the ratio of OTA-APT:OTA-cAPT, concentrations of OTA-cAPT, and OTA-RNA probes, were optimized. As shown in Fig. 2A, the fluorescence signal was strongly dependent on the ratio of OTA-APT to OTA-cAPT, the optimum ratio being achieved at a molar ratio of 3:1. It is supposed that a low amount of OTA-APT would result in unstable OTA-APT/OTA-cAPT duplexes while an excess of OTA-APT would increase the concentration of OTA in OTA-cAPT (Chen et al., 2012). Therefore, the OTA-APT to OTA-cAPT ratio of 3:1 was used for further experiments. Using this optimum ratio, the influence of the concentrations of OTA-cAPT was investigated. The calculated fluorescence ratio, F/F_0, as a function of concentration, is illustrated in Fig. 2B. It can be observed that the fluorescence increases proportionally with the concentration of OTA-cAPT up to 50 nM (namely, 150 nM of OTA-APT), then drastically decreases. This is because there will be excess OTA-cAPT reacting with OTA-RNA due to too high concentration of OTA-cAPT, resulting in an increase in background. Moreover, Fig. 2C shows that the rate at which the fluorescence increases is related to the concentration of OTA-RNA. Thus, the emitted fluorescence continually increases up to a concentration of 300 nM, then it reaches a plateau. Thus, a concentration of 300 nM for OTA-RNA was selected for the subsequent set of experiments.

3.3. Quantitative determination of OTA

Under the optimized conditions, a calibration curve was constructed based on the fluorescence intensity for different concentrations of OTA ranging from 0.08 to 200 ng/mL. The results corresponding to these experiments are illustrated in Fig. 3. As depicted in Fig. 3A, that displays the fluorescence spectra as a function of concentration, the addition of an increasing amount of OTA from 0.08 to 200 ng/mL results in a dynamic increase in fluorescence emission that is centered at 515 nm. According to Fig. 3B that shows the calibration curve of fluorescence intensity as a function of concentration, when OTA concentration is below 40 ng/mL, the fluorescence intensity continuously increases, while further enhancements in the concentration produces only small changes of the intensity and the calibration curve deviates from linearity. In this figure, the linear part of the calibration curve is

also inserted. It reveals that the fluorescence signal is linear with the concentration of OTA in the range from 0.4 to 20 ng/mL. By Origin software analysis, the equation of this curve is F = 6.34C + 269.50, where F is the fluorescence intensity and C is the concentration of OTA (ng/mL) with the square of the correlation coefficient, R^2 of 0.99118 (inset in Fig. 3B). The limit of detection (LOD) was calculated to be 0.08 ng/mL according to signal-to-noise ratio of 3, which is superior or comparable with the previous methods for OTA listed in Table 1. Therefore, it can be concluded that the proposed assay is a simple and straightforward method for the sensitive detection of OTA.

Furthermore, this method can be extended as a universal platform for the assay of other toxins by replacing the sequence of the recognition aptamer.

3.4. Selectivity of OTA assay

The specificity of the method was proven by testing OTB and AFB_1 as well. The experiments were performed using 200 ng/mL concentrations of OTA, OTB or AFB_1. The results are displayed in Fig. 4. It is clear from the Fig. 4 that only OTA can induce a large signal, attributed to the inherent specificity of the aptamer toward OTA (Yu et al., 2018). OTB and AFB_1 emitted only negligible fluorescent signals. Thus, the proposed method is suggested to be a good way of discriminating between OTA and other toxins.

3.5. Determination of OTA in red wine samples

In order to test the feasibility and accuracy of the developed sensor, recovery tests were carried out in red wine samples (Table 2). The aptasensor was used for determining the recoveries of three different concentrations of OTA (0.4, 4, and 12 ng/mL). The recoveries were found to vary from 96.1 to 107.5%, which confirmed the satisfactory accuracy of the assay for targeting OTA in a complex sample (Liu et al., 2018; Wang et al., 2017).

4. Conclusions

In summary, a fluorescence aptasensor was developed for the highly sensitive detection of OTA based on a RNase H-assisted fluorescence amplification strategy. Under optimized conditions, this aptasensor exhibited a low detection limit of 0.08 ng/mL, as well as a linear range from 0.4 to 20 ng/mL OTA, demonstrating excellent performance in comparison with previous reports. At the same time, the interfering mycotoxins in the sample, such as OTB and AFB_1, showed negligible effects on the specificity and sensitivity of the sensor, demonstrating the high selectivity of the proposed sensing system. Furthermore, the aptasensor was applied for the quantitative determination of OTA in red wine with recoveries ranging from 96.1 to 107.5%, which demonstrated that the developed method can be applied to the detection of OTA in real samples. This strategy showed high sensitivity, good selectivity, and therefore, it can be considered as a new approach with applications for the specific detection of various toxins encountered in food and water.

Acknowledgments

This work was supported by National Natural Science Foundation of China (No. 21205142, 31370104), State Key Laboratory of Chemo/Biosensing and Chemometrics, Hunan University (2017006), The Research Innovation Program for Graduates of Central South University (2016zzts580, 2017zzts347).

Conflicts of interest

The authors declare no conflict of interest.

References

Ahmed, N. E., Farag, M. M., Soliman, K. M., Abdel-Samed, A. K. M., & Naguib, K. M. (2007). Evaluation of methods used to determine ochratoxin A in coffee beans. *Journal of Agricultural and Food Chemistry, 55*, 9576–9580.
Alonso-Lomillo, M. A., Domínguez-Renedo, O., Román, T. D., & Arcos-Martínez, M. J. (2011). Horseradish peroxidase-screen printed biosensors for determination of ochratoxin A. *Analytica Chimica Acta, 688*, 49–53.
Assaf, H., Azouri, H., & Pallardy, M. (2004). Ochratoxin A induces apoptosis in human lymphocytes through down regulation of bcl-xl. *Toxicological Sciences, 79* 335-244.
Bennett, J. W., & Klich, M. (2003). Mycotoxins. *Clinical Microbiology Reviews, 16*, 497–516.
Boorman, G. A., Hong, H. L., Dieter, M. P., Hayes, H. T., Pohland, A. E., & Stack, M. (1984). Myelotoxicity and macrophage alteration in mice exposed to ochratoxin A. *Toxicology & Applied Pharmacology, 72*, 304–312.
Chen, J., Fang, Z., Liu, J., & Zeng, L. (2012). A simple and rapid biosensor for ochratoxin A based on a structure-switching signaling aptamer. *Food Control, 25*, 555–560.
Cho, E. J., Lee, J. W., & Ellington, A. D. (2009). Applications of aptamers as sensors. *Annual Review of Analytical Chemistry, 2*, 241–264.
Costa, J. G., Saraiva, N., Guerreiro, P. S., Louro, H., Silva, M. J., Miranda Castro, J. P. M., Batinic-Haberle, I., Fernandes, A. S., & Oliveira, N. G. (2016). Ochratoxin A-induced cytotoxicity, genotoxicity and reactive oxygen species in kidney cells: An integrative approach of complementary endpoints. *Food and Chemical Toxicology, 87*, 65–76.
Feng, J., Li, Y., Gao, Z., Lv, H., Zhang, X., Fan, D., & Wei, Q. (2018). Visible-light driven label-free photoelectrochemical immunosensor based on TiO_2/S-$BiVO_4$@Ag_2S nanocomposites for sensitive detection OTA. *Biosensors and Bioelectronics, 99*, 14–20.
Ghali, R., Hmaissia-Khlifa, K., Ghorbel, H., Maaroufi, K., & Hedili, A. (2008). Incidence ofaflatoxins, ochratoxin A and zearalenone in Tunisian foods. *Food Control, 19*, 921–924.
Ghali, R., Hmaissia-Khlifa, K., Ghorbel, H., Maaroufi, K., & Hedili, A. (2009). HPLC determination of ochratoxin A in high consumption Tunisian foods. *Food Control, 20*, 716–720.
Guo, L., & Zhao, Q. (2016). Thrombin-linked aptamer assay for detection of platelet derived growth factor bb on magnetic beads in a sandwich format. *Talanta, 158*, 159–164.
Imperato, R., Campone, L., Piccinelli, A. L., Veneziano, A., & Rastrelli, L. (2011). Survey of aflatoxins and ochratoxin A contamination in food products imported in Italy. *Food Control, 22*, 1905–1910.
International Agency on Research on Cancer (1993). Some naturally occurring substances: Food items and constituents, heterocyclic aromatic amines and mycotoxins. *Carcinogenic Risk to Humans, 56*, 445–466.
Jo, E. J., Mun, H., Kim, S. J., Shim, W. B., & Kim, M. G. (2016). Detection of ochratoxin a (OTA) in coffee using chemiluminescence resonance energy transfer (CRET) aptasensor. *Food Chemistry, 194*, 1102–1107.
Khoury, A. E., & Atoui, A. (2010). Ochratoxin A: General overview and actual molecular status. *Toxins, 2*, 461–493.
Lea, T., Steien, K., & Størmer, F. C. (1989). Mechanism of ochratoxin A-induced immunosuppression. *Mycopathologia, 107*, 153–159.
Lee, J., Jeon, C. H., Ahn, S. J., & Ha, T. H. (2014). Highly stable colorimetric aptamer sensors for detection of ochratoxin a through optimizing the sequence with the covalent conjugation of hemin. *Analyst, 139*, 1622–1627.
Li, L., Zhao, H., Chen, Z., Mu, X., & Guo, L. (2011). Aptamer biosensor for label-free square-wave voltammetry detection of angiogenin. *Biosensors and Bioelectronics, 30*, 261–266.
Liu, B., Tsao, Z., Wang, J., & Yu, F. (2008). Development of a monoclonal antibody against ochratoxin A and its application in enzyme-linked immunosorbent assay and gold nanoparticle immunochromatographic strip. *Analytical Chemistry, 80*, 7029–7035.
Liu, R., Wu, H., Lv, L., Kang, X., Cui, C., Feng, J., & Guo, Z. (2018). Fluorometric aptamer based assay for ochratoxin A based on the use of exonuclease III. *Microchimica Acta, 185*, 254–259.
Luan, Y., Chen, J., Li, C., Xie, G., Fu, H., Ma, Z., & Lu, A. (2015). Highly sensitive colorimetric detection of ochratoxin A by a label-free aptamer and gold nanoparticles. *Toxins, 7*, 5377–5385.
Lv, L., Li, D., Cui, C., Zhao, Y., & Guo, Z. (2017). Nuclease-aided target recycling signal amplification strategy for ochratoxin A monitoring. *Biosensors and Bioelectronics, 87*, 136–141.
Mayorga-Martinez, C. C., Quesada-González, D., Zamora-Gálvez, A., de la Escosura-Muñiz, A., & Merkoçi, A. (2015). Label-free impedimetric aptasensor for ochratoxin-A detection using iridium oxide nanoparticles. *Analytical Chemistry, 87*, 5167–5172.
Mckeague, M., Velu, R., Hill, K., Bardóczy, V., Mészáros, T., & Derosa, M. C. (2014). Selection and characterization of a novel DNA aptamer for label-free fluorescence biosensing of ochratoxin a. *Toxins, 6*, 2435–2452.
Mishra, R. K., Hayat, A., Catanante, G., Istamboulie, G., & Marty, J. L. (2016). Sensitive quantitation of ochratoxin a in cocoa beans using differential pulse voltammetry based aptasensor. *Food Chemistry, 192*, 799–804.
Muller, G., Burkert, B., & Rosner, H. H. (2003). Effects of the mycotoxin ochratoxin a and some of its metabolites on human kidney cell lines. *Toxicology in Vitro, 17*, 441–448.
Song, C., Hong, W., Zhang, X., & Lu, Y. (2018). Label-free and sensitive detection of Ochratoxin A based on dsDNA-templated copper nanoparticles and exonuclease-catalyzed target recycling amplification. *Analyst, 143*, 1829–1834.
Songsermsakul, P., & Razzazi-Fazelib, E. (2008). A review of recent trends in applications of liquid chromatography-mass spectrometry for determination of mycotoxins. *Journal of Liquid Chromatography & Related Technologies, 31*, 1641–1686.
Studerrohr, I., Schlatter, J., & Dietrich, D. R. (2000). Kinetic parameters and

intraindividual fluctuations of ochratoxin A plasma levels in humans. *Archives of Toxicology, 74*, 499–510.
Tong, P., Zhao, W. W., Zhang, L., Xu, J. J., & Chen, H. Y. (2012). Double-probe signal enhancing strategy for toxin aptasensing based on rolling circle amplification. *Biosensors and Bioelectronics, 33*, 146–151.
Turner, N. W., Subrahmanyam, S., & Piletsky, S. A. (2009). Analytical methods for determination of mycotoxins: A review. *Analytica Chimica Acta, 632*, 168–180.
Van, D. M. K. J., Steyn, P. S., Fourie, L., Scott, D. B., & Theron, J. J. (1965). Ochratoxin a, a toxic metabolite produced by aspergillus ochraceus wilh. *Nature, 205*, 1112–1113.
Wang, B., Wu, Y., Chen, Y., Weng, B., Xu, L., & Li, C. (2016). A highly sensitive aptasensor for ota detection based on hybridization chain reaction and fluorescent perylene probe. *Biosensors and Bioelectronics, 81*, 125–130.
Wang, S., Zhang, Y., Pang, G., Zhang, Y., & Guo, J. (2017). Tuning the aggregation/disaggregation behavior of graphene quantum dots by structure-switching aptamer for high-sensitivity fluorescent ochratoxin A sensor. *Analytical Chemistry, 89*, 1704–1709.
Wu, K., Ma, C., Liu, H., He, H., Zeng, W., & Wang, K. (2017). Label-free fluorescence assay for rapid detection of RNase H activity based on Tb^{3+}-induced Gquadruplex conjugates. *Analytical Methods, 9*, 3055–3060.
Xu, X., Xu, C., & Ying, Y. (2016). Aptasensor for the simple detection of ochratoxin a based on side-by-side assembly of gold nanorods. *RSC Advances, 6*, 50437–50443.
Yang, C., Lates, V., Prieto-Simón, B., Marty, J. L., & Yang, X. (2012). Aptamer-dnazyme hairpins for biosensing of ochratoxin a. *Biosensors and Bioelectronics, 32*, 208–212.
Yin, X., Wang, S., Liu, X., He, C., Tang, Y., Li, Q., ... Dong, Y. (2017). Aptamer-based colorimetric biosensing of ochratoxin a in fortified white grape wine sample using unmodified gold nanoparticles. *Analytical Sciences, 26*, 2724–2727.
Yu, X., Lin, Y., Wang, X., Xu, L., Wang, Z., & Fu, F. (2018). Exonuclease-assisted multicolor aptasensor for visual detection of ochratoxin A based on G-quadruplex-hemin DNAzyme-mediated etching of gold nanorod. *Microchimica Acta, 185*, 259–267.
Zejli, H., Yugender Goud, K., & Marty, J. L. (2018). Label free aptasensor for ochratoxin A detection using polythiophene-3-carboxylic acid. *Talanta, 185*, 513–519.
Zhang, Z., Gan, F., Xue, H., Liu, Y., Huang, D., Khan, A. Z., ... Huang, K. (2016). *Experimental and Toxicologic Pathology, 68*, 205–213.